

Supplementary Information

Intratumoral delivery of engineered recombinant modified vaccinia virus Ankara expressing Flt3L and OX40L generates potent antitumor immunity through activating the cGAS/STING pathway and depleting tumor-infiltrating regulatory T cells

Ning Yang^{1#}, Yi Wang^{1#}, Shuaitong Liu¹, Joseph M. Luna³, Gregory Mazo¹, Adrian Tan⁴, Tuo Li⁴, Jiahu Wang⁵, Wei Yan⁶, John Choi⁶, Anthony Rossi^{1,2}, Jenny Zhaoying Xiang⁴, Charles M. Rice³, Taha Merghoub^{2,7,8}, Jedd D. Wolchok^{2,7,8}, and Liang Deng^{1,2,8*}

¹Dermatology Service, Department of Medicine, Memorial Sloan Kettering Cancer Center, New York, NY 10065, USA.

²Weill Cornell Medical College, New York, NY 10065

³The Laboratory of Virology and Infectious Disease, The Rockefeller University, New York, NY, 10065

⁴Genomic Resources Core Facility, Weill Cornell Medical College, New York, NY, 10065, USA

⁵Genvira Biosciences, Ottawa, ON K1V 1C1, Canada

⁶IMVAQ Therapeutics, Sammamish, WA, 98021, USA

⁷Immuno-oncology service, Human Oncology and Pathogenesis Program; Memorial Sloan Kettering Cancer Center, New York, NY 10065, USA

⁸Parker Institute for Cancer Immunotherapy, Memorial Sloan Kettering Cancer Center, New York, NY

*corresponding author. Mailing address for Liang Deng: Dermatology Service, Department of Medicine, Memorial Sloan Kettering Cancer Center, 1275 York Ave., New York, NY 10065. Email: dengl@mskcc.org. # These two authors contributed equally to this work.

This file contains:

- Supplementary Figure 1
- Supplementary Figure 2
- Supplementary Figure 3
- Supplementary Figure 4
- Supplementary Figure 5
- Supplementary Figure 6
- Supplementary Table 1

Figure S1

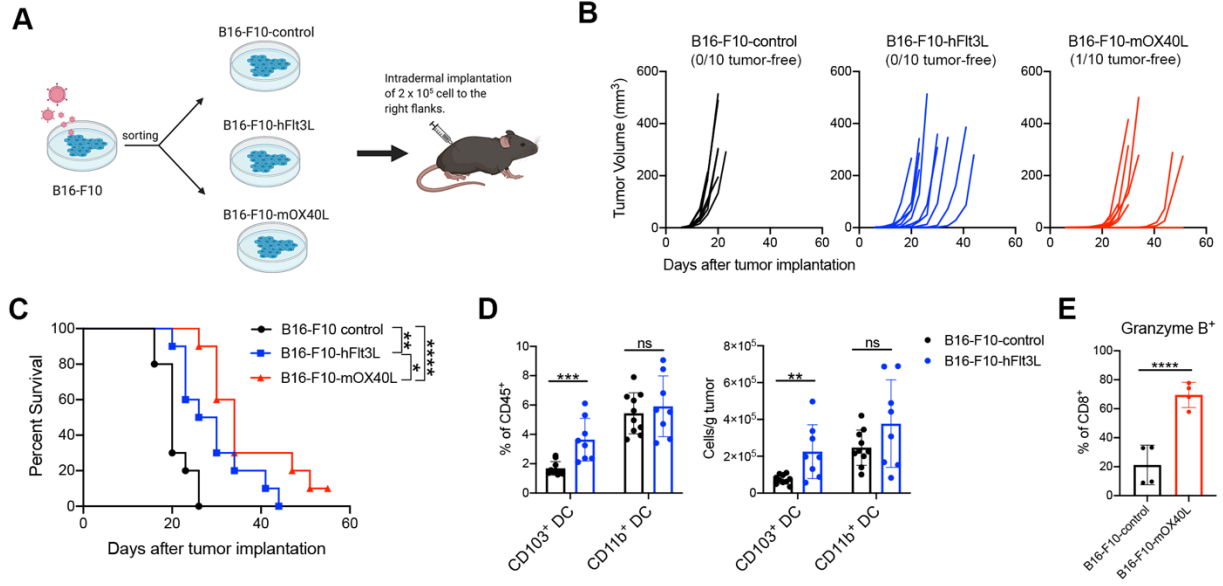


Figure S1. Overexpression of human Flt3L or murine OX40L on B16-F10 tumor cells enhances immunogenicity of the tumors.

(A) B16-F10 were transduced with retrovirus to generate hFlt3L or mOX40L-expressing stable cell lines. C57BL/6J mice were intradermally implanted with 2×10^5 B16-F10-hFlt3L, B16-F10-mOX40L or B16-F10 control cells.

(B) Tumor growth curve ($n=10$).

(C) Kaplan-Meier survival curve ($n=10$; $*P < 0.05$, $**P < 0.01$, $****P < 0.0001$, *Mantel-Cox test*).

(D) Percentages and absolute number of CD103⁺ DCs and CD11b⁺ DCs in B16-F10-hFlt3L or B16-F10-control tumors. Data are means \pm SD ($n=8$ or 10 ; $**P < 0.01$, $***P < 0.001$, *t test*).

(E) Percentages Granzyme B⁺ CD8⁺ and Granzyme B⁺ CD4⁺ in B16-F10-hFlt3L or B16-F10-control tumors. Data are means \pm SD ($n=4$; $****P < 0.0001$, *t test*).

Figure S2

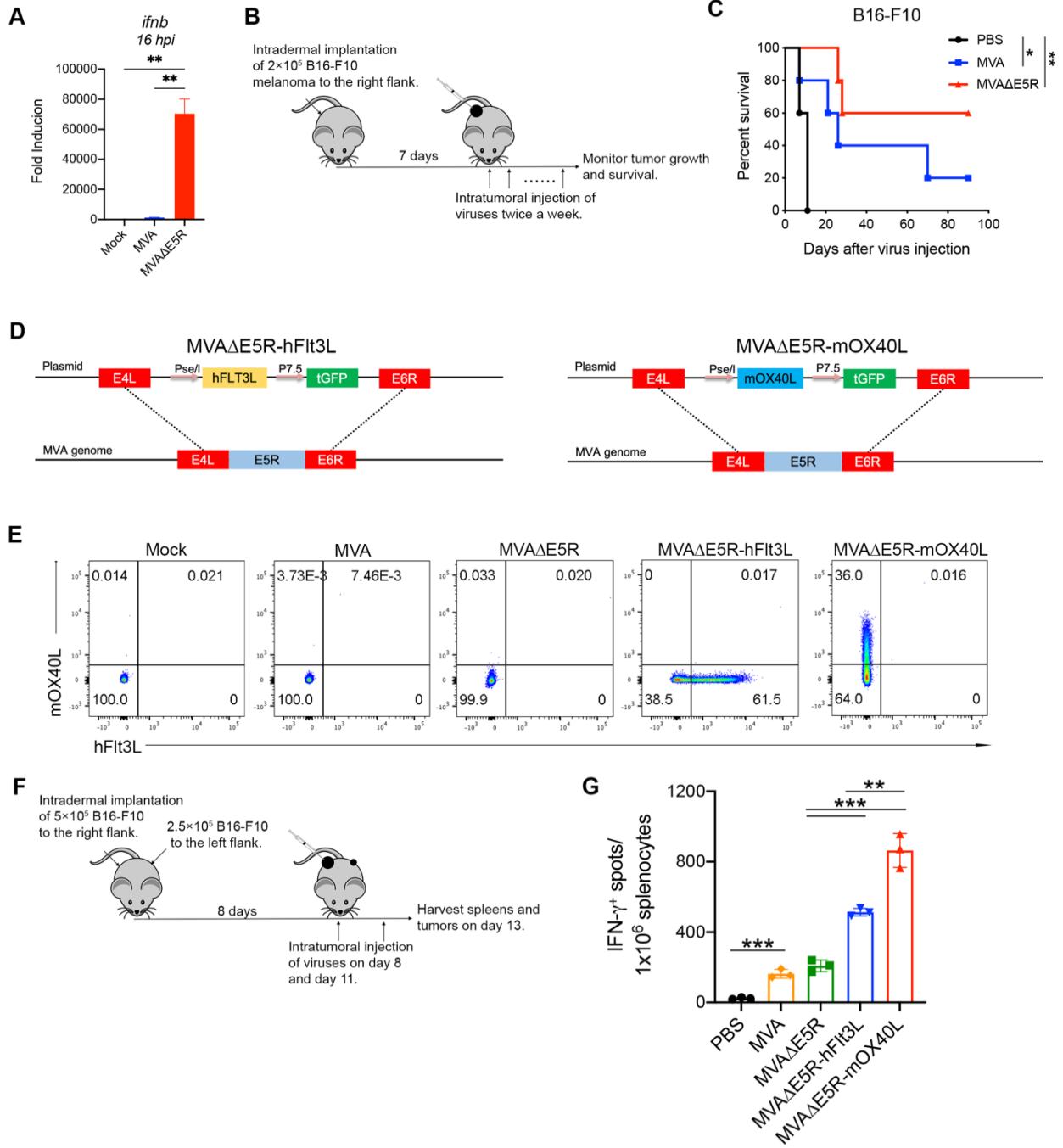


Figure S2. Incremental engineering of MVA with deletion of E5R gene and expression of human Flt3L or murine OX40L improves antitumor effects.

(A) Relative mRNA expression levels of *Ifnb* in BMDCs infected with MVA or MVA Δ E5R. Data are means \pm SD ($n=3$; $**P < 0.01$, *t test*).

(B) Schematic diagram of IT MVA, MVA Δ E5R or PBS in a unilateral B16-F10 melanoma implantation model.

(C) Kaplan-Meier survival curve of mice treated with MVA, MVA Δ E5R or PBS in a unilateral B16-F10 implantation model ($n=10$; $*P < 0.05$, $**P < 0.01$, *Mantel-Cox test*).

(D) Schematic diagrams for the generation of MVA Δ E5R-hFlt3L or MVA Δ E5R-mOX40L through homologous recombination.

(D) Representative flow cytometry plots of expression of hFlt3L or mOX40L by MVA, MVA Δ E5R, MVA Δ E5R-hFlt3L, MVA Δ E5R-mOX40L or mock-infected BHK21 cells.

(E) Representative flow cytometry plots of expression of hFlt3L or mOX40L by MVA, MVA Δ E5R, MVA Δ E5R-hFlt3L, MVA Δ E5R-mOX40L or mock-infected BHK21 cells.

(F) Schematic diagram of IT MVA, MVA Δ E5R, MVA Δ E5R-hFlt3L, MVA Δ E5R-mOX40L or PBS in a bilateral B16-F10 melanoma implantation model.

(G) IFN- γ^+ splenocytes from MVA, MVA Δ E5R, MVA Δ E5R-hFlt3L, MVA Δ E5R-mOX40L or PBS-treated mice. Data are means \pm SD ($n=3$; $*P < 0.05$, $***P < 0.001$, *t test*).

Figure S3

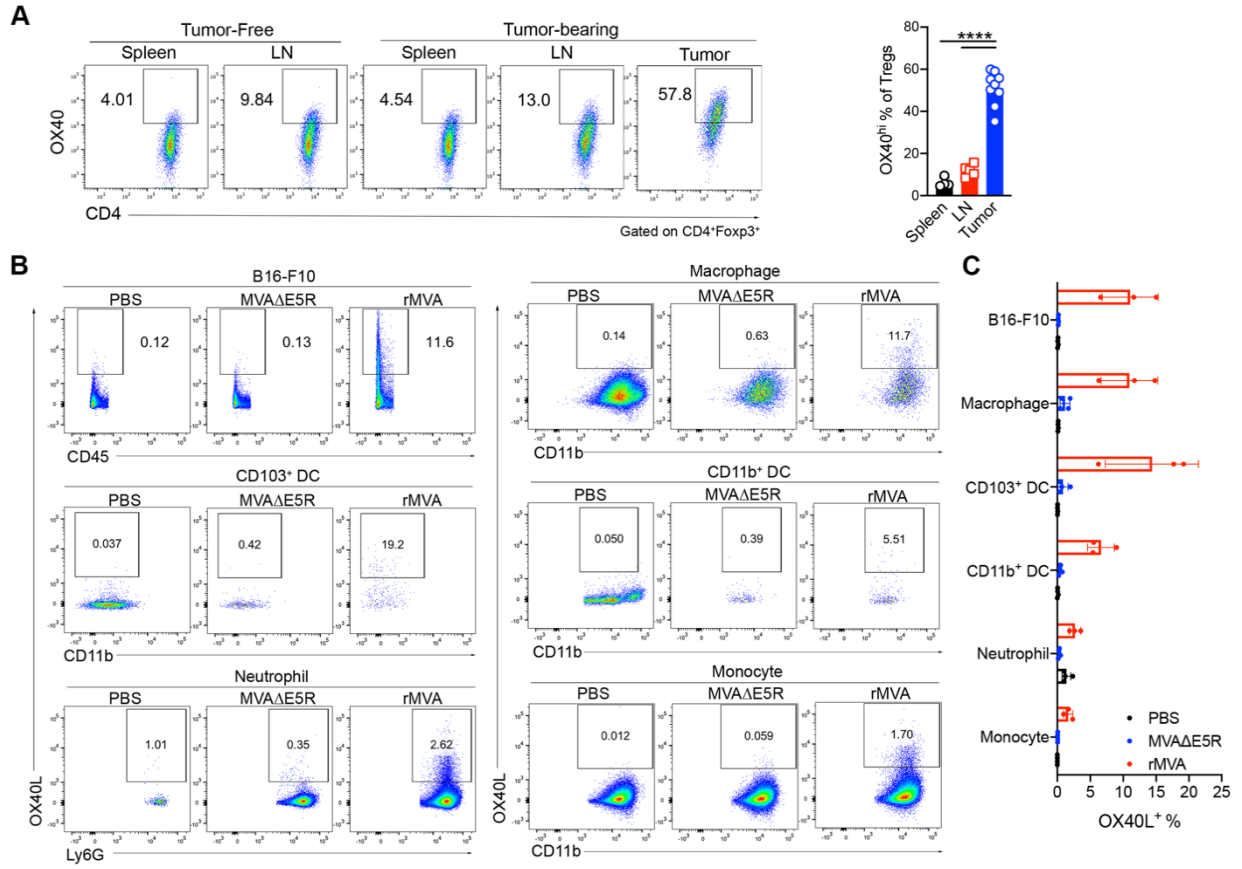


Figure S3. OX40 expression on T cells in lymphoid organs and in tumors and OX40L expression in tumors and tumor-infiltrating cells after IT rMVA.

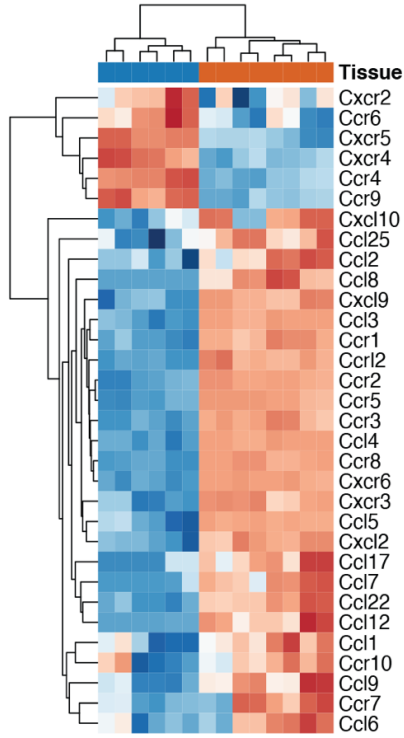
(A) Representative flow cytometry plots of OX40 expression on CD4⁺Foxp3⁺ T cells in the spleens, lymph nodes or tumors from naïve or B16-F10 tumor-bearing mice.

(B) Representative flow cytometry plots of OX40L expression on B16-F10 tumor cells or myeloid cells in the tumors injected with MVAΔE5R, rMVA or PBS as control.

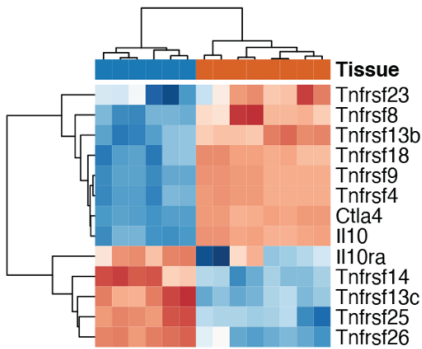
(C) Percentages of OX40L⁺ B16-F10 cells or myeloid cells in the tumors. Data are means ± SD ($n=3\sim5$).

Figure S4

A OX40^{hi} Tumor versus spleen
Chemokines & receptors



B OX40^{hi} Tumor versus spleen
Immune suppressors



C OX40^{hi} Tumor versus spleen
GO Oxidative Phosphorylation

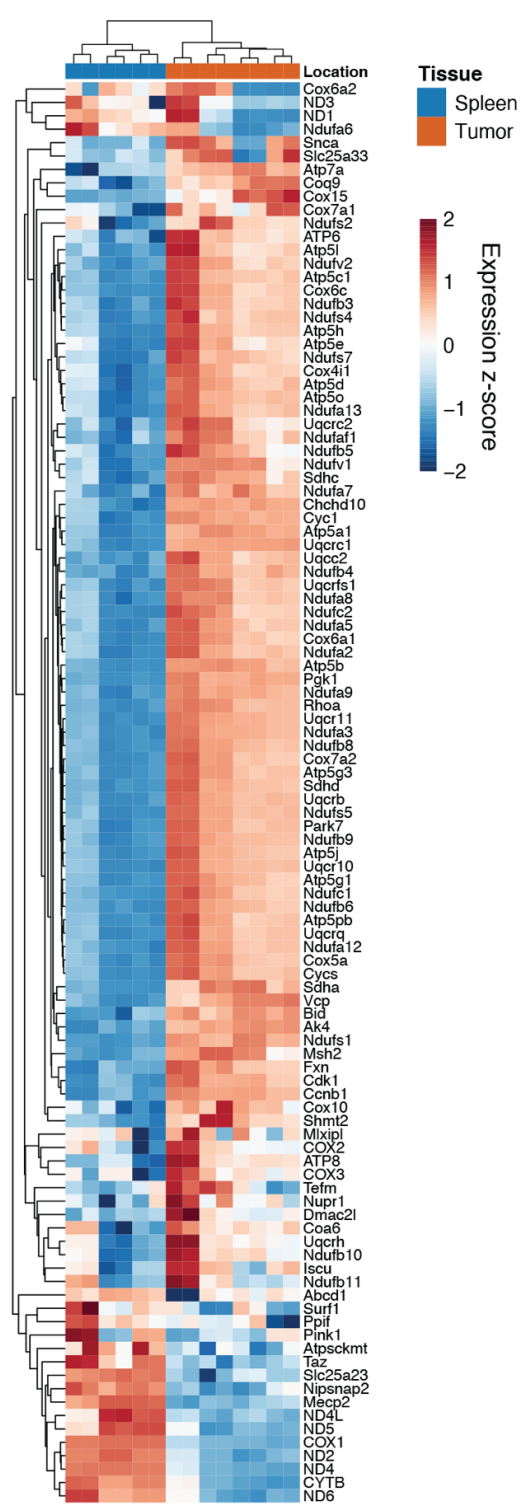


Figure S4. Heatmaps of differential gene expression in OX40^{hi} Tregs isolated from tumors vs. those from spleens.

- (A) Differential gene expression of chemokines and chemokine receptors
- (B) Differential gene expression of immune suppressive genes
- (C) Differential gene expression of genes involved in oxidative phosphorylation.

Figure S5

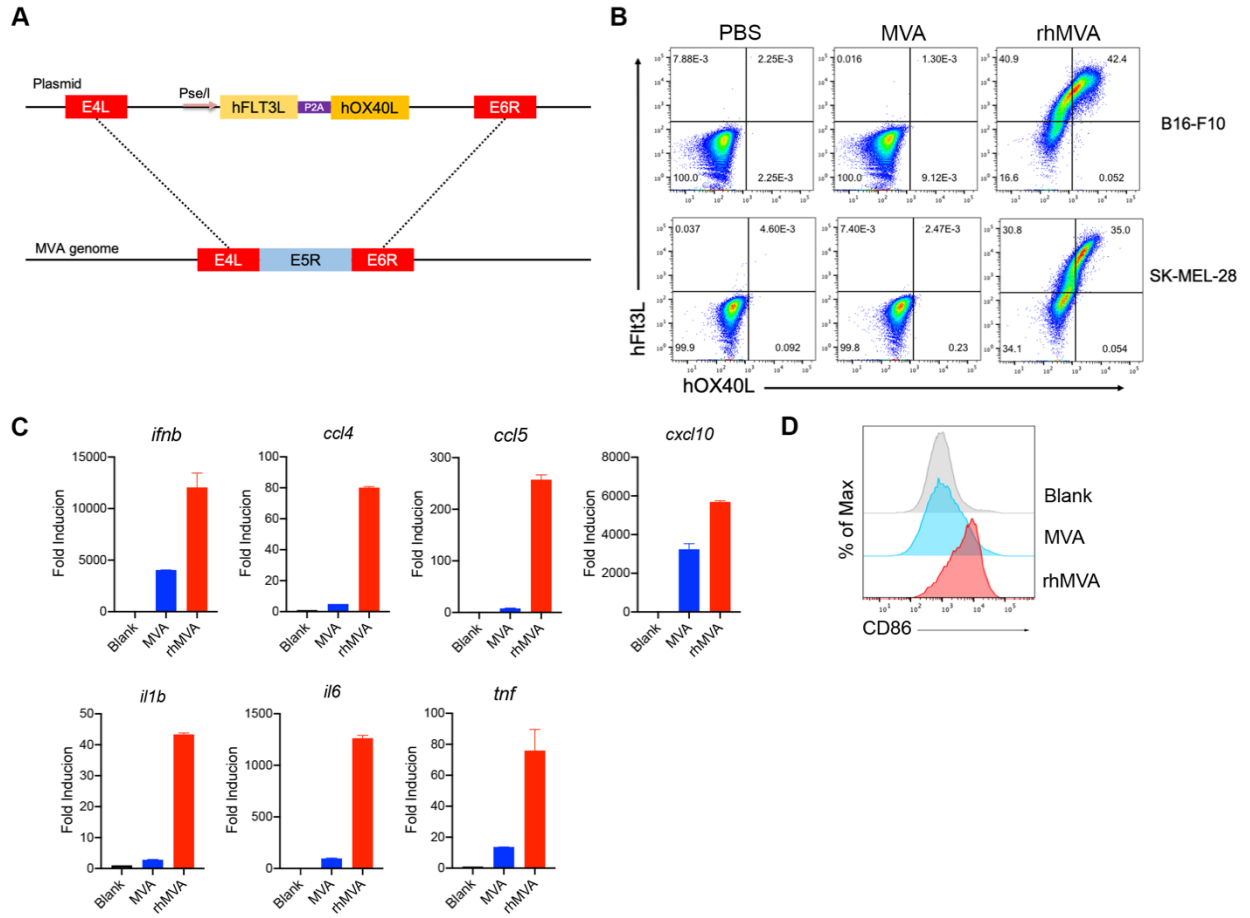


Figure S5. Clinical candidate rhMVA induces innate immunity and promotes maturation of human monocyte-derived DCs (moDCs).

- (A) Schematic diagram for the generation of rhMVA through homologous recombination.
- (B) Representative flow cytometry plots of expression of hFlt3L or hOX40L by rMVA-infected B16-F10 cells and SK-MEL-28 cells.
- (C) Relative mRNA expression levels of *ifnb*, *ccl4*, *ccl5*, *cxcl10*, *il1b*, *il6* and *tnf* in moDCs infected with MVA or rhMVA.
- (D) Mean fluorescence intensity of CD86 expressed by MoDCs infected with MVA or rhMVA.

Figure S6

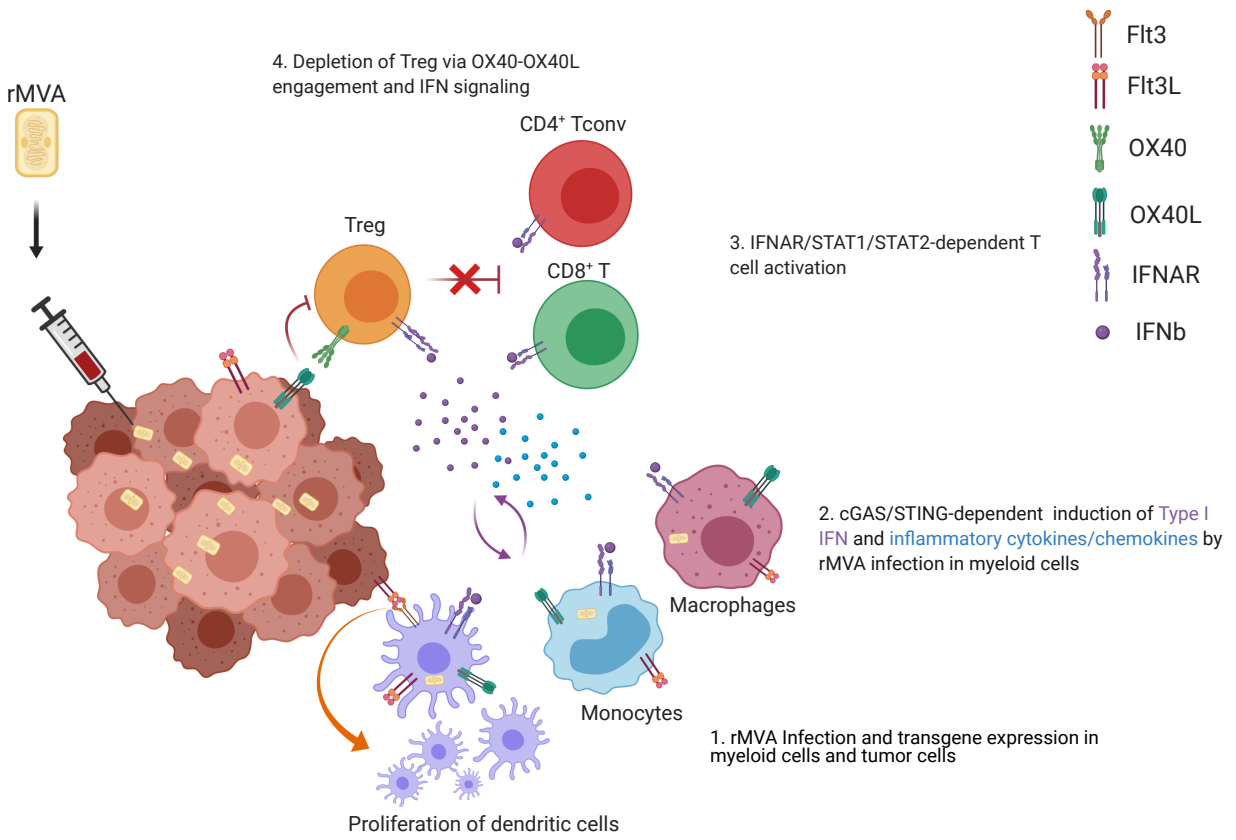


Figure S6. Working model. IT injection of rMVA results in the infection of tumor-infiltrating myeloid cells, including macrophages, monocytes, and dendritic cells, as well as tumor cells. This leads to the activation of cGAS/STING-mediated cytosolic DNA-sensing pathway and the production of type I IFN and cytokines and chemokines that are important for CD8⁺ and CD4⁺ T cell proliferation and activation (as indicated by Granzyme B, TNF, and IFN- γ expression). Flt3L expression of the tumor microenvironment facilitates the proliferation of CD103⁺ DCs in the tumors. OX40L expression by myeloid cell populations and tumor cells results in the depletion of OX40^{hi} Tregs infiltrating the tumors via OX40L-OX40 ligation, which is promoted by type I IFN. This leads to the blunting of their inhibition on tumor-specific effector CD4⁺ and CD8⁺ T cells. Taken together, IT delivery of rMVA results in the alteration of tumor immunosuppressive microenvironment through activation of innate immunity and boosting of antitumor T cells by depletion of OX40^{hi} regulatory T cells.

Table S1. Primers for Real-time PCR

Species	Gene	Direction	Sequence
Mouse	ccl4	Forward	5'-GCCCTCTCTCTCCTCTTGCT-3'
	ccl4	Reverse	5'-CTGGTCTCATAGTAATCCATC-3'
	ccl5	Forward	5'-GCCACGTCAAGGAGTATTTCTA-3'
	ccl5	Reverse	5'-ACACACTTGGCGGTTCCCTTC-3'
	cxcl10	Forward	5'-GTCAGGTTGCCTCTGTCTCA-3'
	cxcl10	Reverse	5'-TCAGGGAAGAGTCTGGAAAG-3'
	cxcl9	Forward	5'-GGAACCCTAGTGATAAGGAATGCA-3'
	cxcl9	Reverse	5'-TGAGGTCTTTGAGGGATTTGTAGTG-3'
	ifna	Forward	5'-CCTGTGTGATGCAGGAACC-3'
	ifna	Reverse	5'-TCACCTCCCAGGCACAGA-3'
	ifnb	Forward	5'-TGGAGATGACGGAGAAGATG-3'
	ifnb	Reverse	5'-TTGGATGGCAAAGGCAGT-3'
	GAPDH	Forward	5'-ATCAAGAAGGTGGTGAAGCA-3'
	GAPDH	Reverse	5'-AGACAACCTGGTCCTCAGTGT-3'
	ccl4	Forward	5'-AAAACCTCTTTGCCACCAATACC-3'
	ccl4	Reverse	5'-GAGAGCAGAAGGCAGCTACTAG-3'
Human	cxcl10	Forward	5'-ATTTGCTGCCTTATCTTTCTG-3'
	cxcl10	Reverse	5'-TCTCACCTTCTTTTTTCATTGTAG-3'
	ifnb	Forward	5'-GCACTGGCTGGAATGAGACT-3'
	ifnb	Reverse	5'-CCTTGGCCTTCAGGTAATG-3'
	il6	Forward	5'-AATTCGGTACATCCTCGACGG-3'
	il6	Reverse	5'-TTGGAAGGTTTCAGGTTGTTTTCT-3'
	tnf	Forward	5'-AATAGGCTGTTCCCATGTAGC-3'
	tnf	Reverse	5'-AGAGGCTCAGCAATGAGTGA-3'
	GAPDH	Forward	5'-ATCAAGAAGGTGGTGAAGCA-3'
	GAPDH	Reverse	5'-GTCGCTGTTGAAGTCAGAGGA-3'